ISSN 2682-681X (Paper), ISSN 2705-4241 (Online) | http://unilorinjoger.com | https://doi.org/10.63745/jogersi.2026.06.30.005

JOGER SPECIAL ISSUE, 2026
JOURNAL OF GEOMATICS AND ENVIRONMENTAL RESEARCH http://www.unilorinjoger.com

Flood Detection and Mapping Using Sentinel-1 SAR Data: A Case Study of the Confluence Region of Kogi State, Nigeria

Hussein Adomu Ahmadu[1*], Ayo Babalola[2] & Oluwafemi Oyetunde Adeleke[3]

[1-2,] Department of Surveying and Geoinformatics, Faculty of Environmental Sciences, University of Ilorin, Nigeria.
[3]Department of Civil Engineering, Faculty of Engineering and Technology, University of Ilorin, Nigeria.

*ahmadu.ha@unilorin.edu.ng | https://orcid.org/0009-0009-9402-3417

Abstract

Flooding remains one of the most recurrent and destructive natural hazards affecting communities within the Niger–Benue confluence region of Kogi State, Nigeria. Accurate and timely information on flood extent is essential for disaster preparedness, emergency response, and sustainable flood risk management. This study employed multi-temporal Sentinel-1 Synthetic Aperture Radar (SAR) imagery to detect and map flood inundation associated with major flood events in 2018, 2020, 2022, and 2024 within the confluence region of Kogi State. Sentinel-1 Ground Range Detected (GRD) datasets acquired before and during flood events were processed using the Google Earth Engine (GEE). Image processing involved sub-setting, orbit file correction, radiometric calibration, Noise removal, speckle filtering, terrain correction, and decibel conversion. A threshold-based image binarization was used to distinguish floodwaters from permanent water bodies (flood extent extraction). The resulting flood maps were analyzed in ArcGIS Pro to calculate flood extent area, while Moran's spatial statistics were used to analyze the spatial pattern of flood for all the years considered. Also, the flood maps were overlaid on land use land cover maps to determine the impact of flooding in the study area, while a flood density map was produced in ArcGIS Pro to reveal flood hotspots and flood-prone areas within the study area. Results revealed significant expansion of floodwaters along the Niger and Benue floodplains, with varying levels of inundation observed across the investigated flood events. Also, the areas most impacted by flood waters were mainly farmlands and built-up areas close to the banks of the River Niger. The findings demonstrated the effectiveness of Sentinel-1 SAR imagery for flood monitoring under all-weather conditions and highlighted its potential for supporting flood early warning systems, disaster management, and resilience planning within flood-prone regions of Nigeria.

ARTICLE INFORMATION
Received: 18 May 2026
Revised: 30 May 2026
Accepted: 30 June 2026
Published: 20 July 2026

KEYWORDS
Flood Mapping, Sentinel-1 SAR, Synthetic Aperture Radar, Flood Detection, Remote Sensing, Kogi State, Niger-Benue Confluence.
.

Citation: Ahmadu, H. A., Babalola. A. & Adeleke O.O. (2026). Flood Detection and Mapping Using Sentinel-1 SAR Data: A Case Study of the Confluence Region of Kogi State, Nigeria**.** Journal *of Geomatics and Environmental Research*, Special Issue 1(1), Pp 64-79.

1.0 INTRODUCTION

Flooding is one of the most frequent and devastating natural hazards worldwide, causing substantial loss of life, destruction of infrastructure, environmental degradation, displacement of populations, and disruption of socio-economic activities (Rahman *et al*., 2025; Hategekimana *et al*., 2026). The increasing frequency and intensity of flood events have been attributed to climate change, rapid urbanization, land-use change, population growth, and inadequate drainage infrastructure (Acosta-Coll *et al*., 2018; Tang *et al*., 2026). Globally, floods affect millions of people annually and account for a significant proportion of disaster-related economic losses (Mazarakis *et al*., 2025).

In Nigeria, flooding has become a recurring environmental challenge with severe impacts on settlements, transportation networks, agricultural production, public infrastructure, and economic development (GFDRR, 2013; UNDP, 2023). Major flood events recorded in 2012, 2018, 2022, and 2024 caused widespread devastation across several states, particularly those located within the Niger–Benue River Basin (UNDP, 2023; Ohunene *et al*., 2025). Communities situated along major river systems remain highly vulnerable because of their proximity to floodplains, low-lying topography, and exposure to seasonal river overflow (Okosun *et al*., 2025). The recurring nature of these events underscores the need for effective flood monitoring and evidence-based flood management strategies.

Accurate flood extent information forms the foundation of effective flood risk management (Wang *et al*., 2022). Flood maps are essential for identifying vulnerable areas, supporting emergency response operations, planning evacuation routes, assessing infrastructure exposure, and informing land-use planning decisions (Shuaibu *et al*., 2022). Furthermore, flood extent maps serve as valuable tools for post-disaster damage assessment, infrastructure planning, evacuation planning, and flood risk modelling (Bhola *et al*., 2020; Destefanis *et al*., 2025). Over the years, numerous flood mapping techniques have been developed, ranging from conventional field surveys and hydraulic modelling approaches to modern geospatial and remote sensing methods (Kumar *et al*., 2023; Sampson *et al*., 2015).

Traditional flood mapping approaches often rely on hydrological observations, hydraulic simulations, and field surveys (Kumar *et al*., 2023; Sampson *et al*., 2015). Although these methods provide valuable information, they are often expensive, labour-intensive, time-consuming, and difficult to implement over large geographical areas during active flood events (Chlumsky *et al*., 2025; Nazir *et al*., 2025). Advances in Geographic Information Systems (GIS) and remote sensing technologies have significantly enhanced flood monitoring capabilities through rapid acquisition and analysis of spatial information.
Optical remote sensing systems such as Landsat and Sentinel-2 have been extensively used for flood detection (Samela *et al*., 2022). However, optical imagery is frequently affected by cloud cover, atmospheric conditions, and illumination constraints during flood events (Wang *et al*., 2019). Since floods commonly occur during periods of intense rainfall, cloud cover often limits the effectiveness of optical imagery when timely information is most needed.

Synthetic Aperture Radar (SAR) technology provides an effective alternative for flood monitoring because microwave signals can penetrate clouds and acquire imagery regardless of weather conditions or time of day (Lang *et al*., 2024; Martinis, 2010). These characteristics make SAR imagery particularly suitable for rapid flood detection and disaster response applications.

Among available SAR missions, Sentinel-1 provides free and openly accessible C-band SAR imagery with high temporal resolution, making it one of the most widely used datasets for operational flood monitoring worldwide. Numerous studies have demonstrated the capability of Sentinel-1 SAR imagery for accurately delineating flood extents under adverse weather conditions. For example, Lang *et al*., (2024) Applied automatic thresholding and change detection on SAR images to map floods in the Wharfe and Ouse river basin. Sajid *et al*., (2025) Applied an optimal threshold-based classification on SAR images to accurately delineate and map flooded areas in the central region of Bihar. Kaçmaz & Alganci, (2026) developed an attention-based differential Siamese U-Net mechanism utilizing SAR images to detect and map flood extent across forty six flood incidents in six continents. Mason & Dance, (2026) Combined Sentinel-1 SAR data with elevation data, image intensity, and interferometric coherence to detect and map flood extent in Asia and Europe.

The confluence region of Kogi State represents one of the most flood-prone areas in Nigeria due to its location at the meeting point of the Niger and Benue Rivers. The region experiences recurrent flooding resulting from heavy rainfall, upstream river discharge, dam releases, and seasonal hydrological processes (Jimoh, 2022; Patricia *et al*., 2024). Consequently, this frequently affects settlements, agricultural lands, transportation corridors, and economic activities (Jimoh, 2022; Patricia *et al*., 2024). Despite the recurrent nature of flooding in the area, there remains a need for accurate and spatially explicit flood extent information that can support disaster preparedness, emergency response, and long-term flood risk management (Jimoh, 2022). This study seeks to employ Sentinel-1 SAR data for flood detection and mapping in the Confluence Region of Kogi State, with the aim of producing accurate flood extent information that can support flood risk reduction, disaster management, and resilience-building initiatives within the study area.

2.0 MATERIALS AND METHODS

2.1 Study Area

The study area (shown in Figure 1) is located within the confluence region of Kogi State, North-Central Nigeria, where the River Niger and River Benue converge. The study covers portions of Lokoja, Bassa, Kogi, Ajaokuta, and Adavi Local Government Areas, all of which have experienced recurrent flood disasters. Geographically, the study area is located within the latitude: $7^0 41' N$ to Latitude: $7^0 52' N$, and Longitude: $6^0 36' E$ to longitude: $6^0 48' E$. It covers an approximate area of 328 km² and is characterized by extensive floodplains, low-relief terrain, and proximity to major river systems (NIHSA, 2023). The climate is tropical with distinct wet and dry seasons. The rainy season extends from April to October, while the dry season occurs between November and March. The region encompasses an elevation range of 30 to 400m above sea level. The region experiences an average annual temperature of $27^0 C$, and an average annual rainfall that varies from 1000mm to 1500mm each year (Ayuba *et al*, 2021; Ekene *et al*., 2025).

The dominant land-use types include settlements, agricultural lands, riparian vegetation, shrublands, and river channels. The major rivers influencing flooding within the area are the River Niger, River Benue, River Meme, and River Ossara. The study area comprises a range of land cover and vegetation types, including cropland, shrubs, short grasses, and tall trees (Alabi, 2012). Primary economic activities in this region include farming, local industries, and commercial activities like banking and trading (Alabi, 2012)

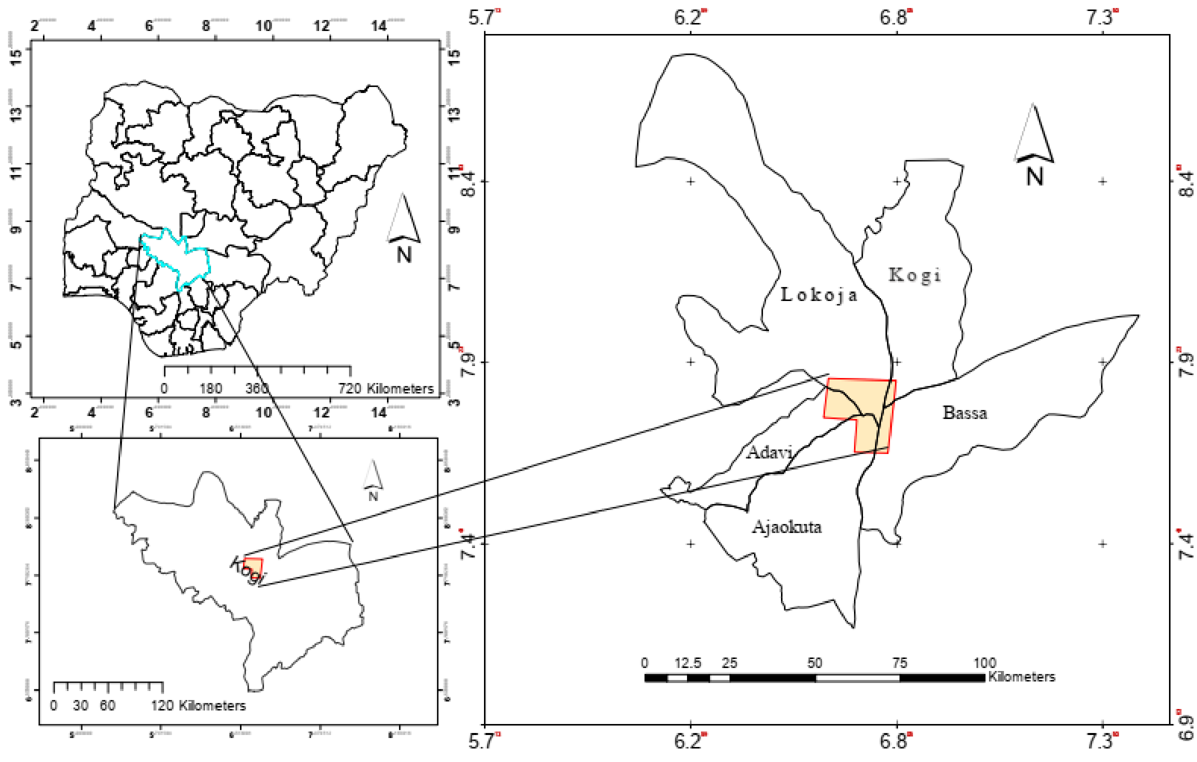

Figure 1. Location map of the Study Area

2.2 Historical Flood Occurrence

The study area has experienced several significant flood events over the past decade. The 2012 flood event remains one of the most devastating in Nigeria's history, while subsequent floods in 2018, 2022, and 2024 caused extensive inundation of settlements, farmlands, and infrastructure. The 2022 flood event was particularly severe due to prolonged rainfall, river overflow, and upstream hydrological influences.

2.3 Data Acquisition

Sentinel-1 SAR Data

Sentinel-1 Ground Range Detected (GRD) imagery was acquired through the GEE platform. The GEE platform has the capability to automatically access and download Sentinel-1 images from Copernicus. Sentinel-1 operates as a C-band SAR mission under the Copernicus Programme and provides imagery suitable for flood monitoring applications (Wagner *et al.*, 2026). The Interferometric Wide Swath (IW) acquisition mode was adopted because it offers a spatial resolution of approximately 10 m and is specifically designed for land monitoring applications (Venter & Sydenham, 2021). The technical specifications of the Sentinel-1 SAR dataset used for this study are presented in Table 1.

Table 1: Technical specifications of the Sentinel-1 SAR imagery dataset used for the flood events considered in this study. The table details the specific scene identifiers and acquisition parameters. All scenes belong to the Ascending orbit track.

Event	Date	Mission	Orbit	UTC	Sentinel-1 Scene ID
1	24/02/18	S1A	Ascending	17:45:33	S1A_IW_GRDH_1SDV_20180224T174533_ 20180224T174558_020752_023902_9A79
2	22/09/18	S1B	Ascending	17:45:03	S1B_IW_GRDH_1SDV_20180922T174503_ 20180922T174528_012831_017B08_5804_3
3	10/05/22	S1A	Ascending	17:45:59	S1A_IW_GRDH_1SDV_20220510T174559_ 20220510T174624_043152_052751_E0E7
4	13/10/22	S1A	Ascending	17:46:07	S1A_IW_GRDH_1SDV_20221013T174607_ 20221013T174632_045427_056EAB_1409
5	4/06/24	S1A	Ascending	17:46:09	S1A_IW_GRDH_1SDV_20240604T174609_ 20240604T174634_054177_0696AE_C6FA
6	26/10/24	S1A	Ascending	17:46:08	S1A_IW_GRDH_1SDV_20241026T174608_ 20241026T174633_056277_06E43D_253F

Extreme flood events recorded in 2018, 2020, 2022, and 2024 were selected for flood extent mapping, due to the fact that they have been the most devastating flood incidents that have affected the confluence region of Kogi State. For each of the years considered, SAR images (Level-1 GRD products) were downloaded for both the archive (pre-flood) and the crisis (post-flood). However, SAR images of the exact flood event dates were not available for download in Sentinel-1 data archives. Only available images close to the exact dates were downloaded and used for this study. Table 2 details the dates of available SAR images downloaded for each flood incident considered in this study.

Table 2: Dates of SAR datasets that were available for download from Sentinel-1 for the flood events

S/N	Flood event Date	Coincident/closest image date available on Sentinel-1 archives
1	21/09/2018	22/09/2018 (1 day after)
	05/10/2020	08/10/2020 (3 days after)
2	4/10/2022	13/10/2022 (9 days after)
3	25/10/2024	26/10/2024 (1 day after)

In this study, detection and mapping of flood inundation from SAR data followed three stages. These include data pre-processing, binarization (extraction of flooded areas), and validation of results. The pre-processing, binarization, and extraction stages were conducted in Google Earth Engine, while validation and analysis were conducted in ArcGIS Pro.

2.4 SAR Image Processing

Data pre-processing enhances data quality and converts the Sentinel-1 SAR VV and VH polarization bands into backscatter values necessary for the identification of water and non-water areas (Sajid *et al.*, 2025). Figure 2 shows the methodological flowchart, with all the stages of SAR data pre-processing. Details of each stage are explained as follows:
The processing workflow is presented in Figure 2.

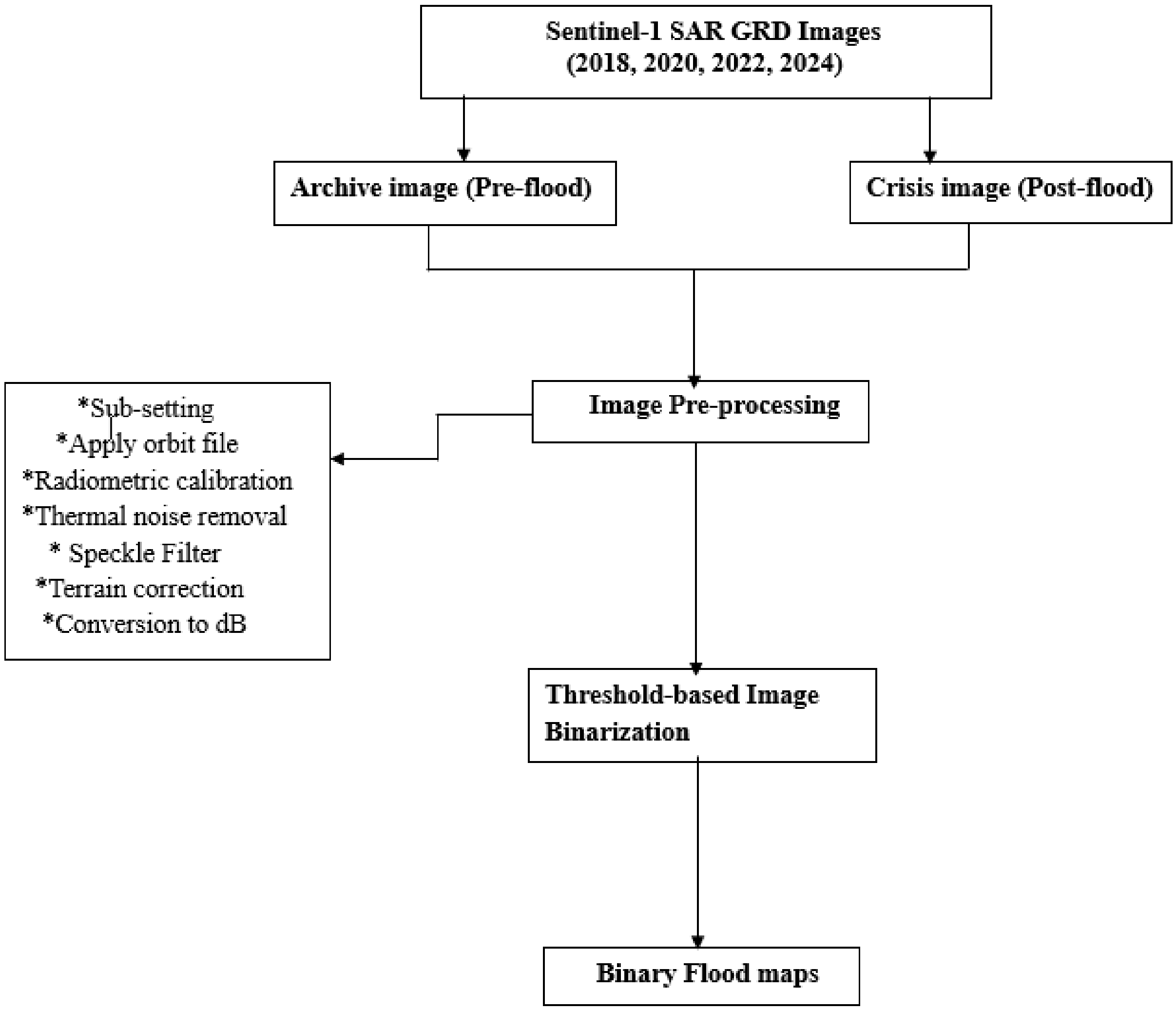

Figure 2: Methodological flowchart for flood detection and mapping from SAR images

2.4.1 Image Sub-setting

The first stage of SAR image preprocessing involved the creation of subsets from both the archive (pre-flood) and crisis (after flood-period) Sentinel-1 images the Google Earth Platform. Sentinel-1 scenes typically cover very large geographical extents, often extending far beyond the boundaries of the study area. Processing the entire scene would therefore require substantial computational resources and processing time while including large amounts of irrelevant information. To address this issue, image sub-setting was performed to extract only the portion of each image corresponding to the confluence region of Kogi State. This was achieved by defining the spatial extent of the study area using a predefined area of interest (AOI) boundary. The resulting subset images contained only the pixels relevant to the study area, thereby eliminating unnecessary data from surrounding regions.

2.4.2 Orbit File Correction

Orbit file correction updates the Sentinel-1 SAR image with precise satellite orbit information to improve its geometric accuracy and positional alignment. This correction ensures that image pixels are accurately georeferenced, thereby enhancing the reliability of subsequent analyses such as flood detection and change analysis (Filipponi, 2019).

2.4.3 Radiometric Calibration

Following image sub-setting, radiometric calibration was performed on both the archive (pre-flood) and crisis (flood-period) Sentinel-1 SAR images using the Calibration tool in SNAP. Radiometric calibration is a critical preprocessing step that transforms the raw digital numbers (DNs) recorded by the SAR sensor into physically meaningful radar backscatter values (Filipponi, 2019). This process establishes a direct relationship between the pixel intensity values and the actual radar energy reflected from the Earth's surface, thereby making the imagery suitable for quantitative analysis and comparison (Zhou *et al*., 2025).

2.4.4 Thermal Noise Removal

Thermal noise removal eliminates sensor-induced noise that appears as unwanted variations in radar backscatter values, particularly in low-backscatter areas and near image edges. Removing this noise improves image radiometric quality and enhances the distinction between water and non-water surfaces, leading to more accurate flood mapping (Filipponi, 2019; ESA, 2023).

2.4.5 Speckle Filtering

Following radiometric calibration, speckle filtering was performed on both the archive (pre-flood) and crisis (flood-period) Sentinel-1 SAR images using the Refined Lee filter. Speckle filtering is an essential preprocessing step in SAR image analysis because SAR imagery is inherently affected by speckle noise, a granular noise pattern caused by the constructive and destructive interference of radar signals reflected from multiple scatterers within a single resolution cell (Jong-Sen Lee *et al*., 2009).

2.4.6 Terrain Correction

Following speckle filtering, terrain correction was performed on the Sentinel-1 SAR images using the Range Doppler Terrain Correction algorithm. Terrain correction is a critical preprocessing step in SAR image analysis because radar images are inherently affected by geometric distortions resulting from the side-looking imaging geometry of the sensor and variations in terrain elevation (Filipponi, 2019). Terrain correction geo-references the SAR imagery and accurately aligns image pixels with their true geographic positions on the Earth's surface.

2.4.7 Conversion of Terrain-Corrected Images to Decibel (dB)

Following terrain correction, the calibrated and georeferenced Sentinel-1 SAR images were converted from linear backscatter values to logarithmic decibels (dB). This step is commonly performed in SAR image processing because radar backscatter values often span a very wide dynamic range, making direct interpretation and visualization of linear values difficult (Twele *et al*., 2016).

2.5 Threshold-based Image Binarization

Binarization is the process of converting a continuous or multi-valued image into a binary image containing only two classes (Gonzalez & Woods, 2018):

$$f(x,y) = \begin{cases} 1, & \text{if } g(x,y) > T \\ 0, & \text{if } g(x,y) \le T \end{cases} \qquad \text{-------------------- (1)}$$

where:

- $g(x,y)$= pixel value in the input image
- T= threshold value
- 1 = foreground/object (flood)
- 0 = background (non-flood)

In this study, a threshold-based image binarization procedure was applied to the SAR change ratio image to separate flooded and non-flooded areas. Pixels with ratio values greater than the selected threshold were assigned a value of 1 (flooded), while pixels below the threshold were assigned a value of 0 (non-flooded), thereby producing a binary flood extent map.

Where the threshold is computed using the SAR ratio image given as;

$$Ratio = \frac{After\ Flood}{Before\ Flood} \qquad \text{-- (2)}$$

2.6 Spatiotemporal Analysis

Based on the flood extent maps, the spatial pattern of floods in the study area was analyzed using Moran's I spatial autocorrelation. Moran's I determines whether spatial data is clustered, dispersed, or randomly distributed (Kumari *et al*., 2019);(Y. Wang *et al*., 2023). It measures the spatial autocorrelation of a set of features by considering both the features' locations and their identified attributes (ESRI, 2020). Moran's spatial autocorrelation can be mathematically expressed as (Chen, 2021); (Chen, 2023):

$$I = \frac{n}{\sum_{i=1}^{n}\sum_{j=1}^{n} w_{ij}} \cdot \frac{\sum_{i=1}^{n}\sum_{j=1}^{n} w_{ij}(x_i - \bar{x})(x_i - \bar{x})}{\sum_{i=1}^{n}(x_i - \bar{x})^2} \quad (3)$$

Where:

n = number of spatial units

x_i = value of the variable location at i

$\bar{x}$ = mean of the variable

w_{ij} = spatial weights that define the relationship between spatial units I and j

It ranges between: $-1 \leq I \leq 1$,

Where;

$\approx +1$ implies a perfect spatial autocorrelation (strong clustering of similar values)

≈ 0 signifies a random spatial pattern (no spatial correlation)

≈ -1 signifies a negative spatial autocorrelation (checkerboard-like dispersion of dissimilar values

In addition, the statistical significance of Moran's index is evaluated using both a z- score and a p–value, where:

Z > 2.58, and p < 0.01 signify strong positive autocorrelation (high clustering)

$z \approx 0, and\ p > 0.05$, signify a random spatial pattern

Z < -2.58, and p < 0.01, signify strong negative autocorrelation (spatial dispersion)

2.6 Flood Density

Flood density map, often referred to as flood frequency or flood occurrence map, reveals how often an area is flooded over time, during recurring flood events. To create the flood density map, the binary flood maps (having 0 to 1 pixel values) were stacked in ArcGIS Pro through a cell-by-cell raster addition. By summing the rasters together using the raster calculator, the resulting pixel values ranged from 0 to 4, where;

- Value 0: Never flooded across all observed dates (permanently dry/safe zones).
- Value 1 or 2: Low density/frequency. Flooded only during extreme or specific events.
- Value 3: High density/frequency. Highly vulnerable, recurrent flood zones.
- Value 4: Flooded during every single mapped observation (potentially permanent water bodies or severe, chronic flood basins).

2.7 Impact assessment

To assess the impact of flooding on the study area between 2018 and 2024, the flood extent maps were overlaid on land use land cover maps to determine the nature and type of land use existing in areas affected by flooding.

2.8 Validation of Results

The reliability of the extracted flood extent maps was evaluated through qualitative validation using historical flood reports and field observations within the study area.

3.0 RESULTS

3.1 Image pre-processing

Image pre-processing was a critical step that enhanced the quality of the Sentinel-1 SAR images and improved their suitability for flood detection and mapping. The preprocessing workflow comprised image sub-setting, orbit correction, thermal and border noise removal, radiometric calibration, speckle filtering, terrain correction, and conversion of backscatter values to the logarithmic decibel (dB) scale. The resulting archive (pre-flood) and crisis (post-flood) images are presented in Figure 3, while the corresponding flood extent maps generated through threshold-based binarization are shown in Figure 4.

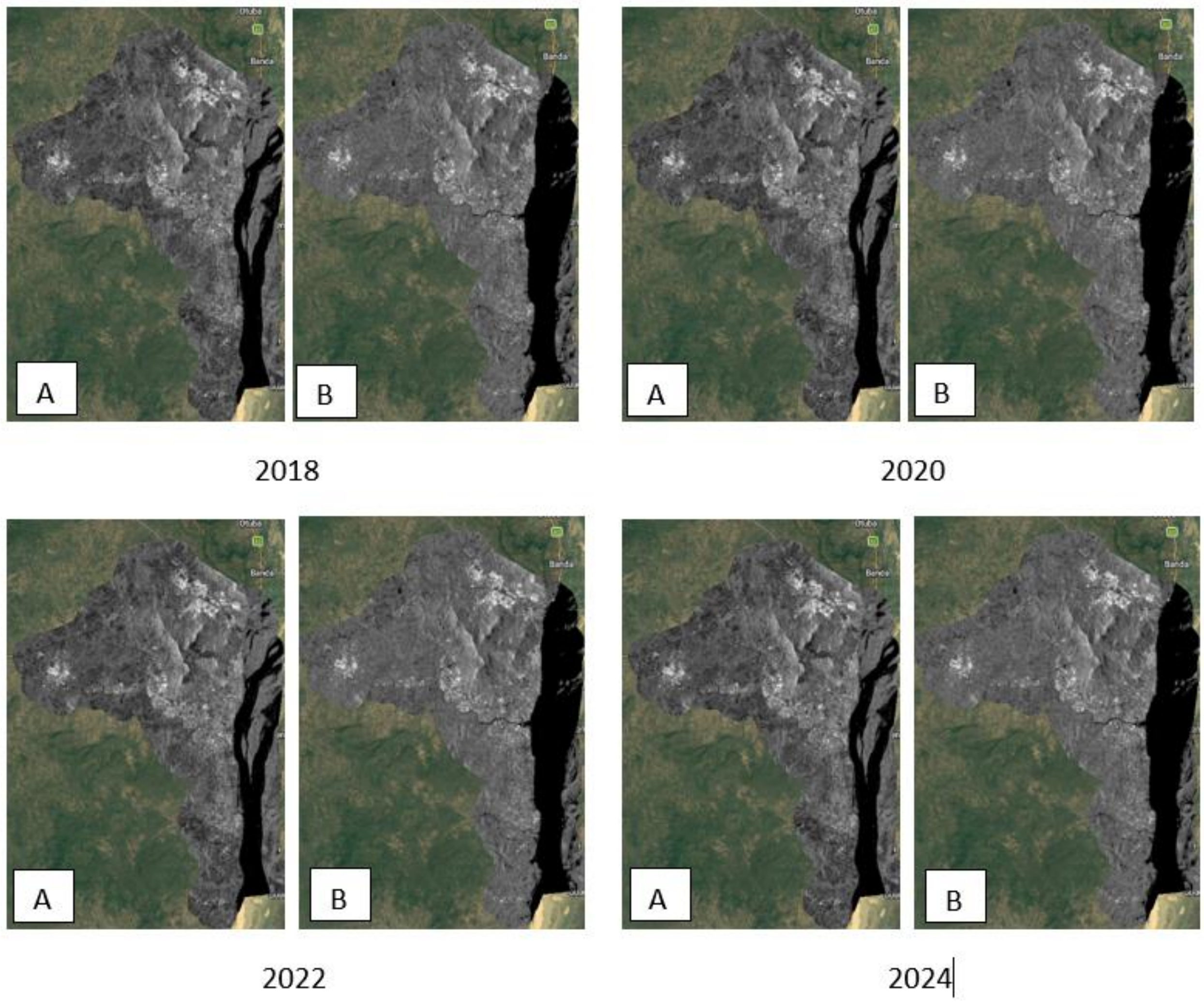

Figure 3. Pre-processed SAR images. A: Archive image (before flood) and B: Crisis image (after flood)

Image sub-setting reduced the Sentinel-1 scenes to the study area, thereby eliminating unnecessary data and improving processing efficiency. Orbit correction and terrain correction enhanced the geometric accuracy of the images by ensuring that both archive and crisis images were correctly aligned and georeferenced, making them suitable for change detection and spatial analysis. Thermal and border noise removal eliminated sensor-induced artefacts, while radiometric calibration converted the raw digital numbers into physically meaningful backscatter values, allowing different surface features to be reliably distinguished based on their radar response.

Speckle filtering using the Refined Lee filter significantly reduced the granular noise inherent in SAR imagery while preserving important feature boundaries. Consequently, permanent water bodies and flooded areas appeared as smooth, dark regions, whereas vegetation, built-up areas, and other rough surfaces exhibited higher backscatter and brighter tones in the pre-processed images (Figure 3). Conversion to the dB scale further enhanced image contrast, making the distinction between water and non-water surfaces more pronounced.

The cumulative effect of these preprocessing operations produced radiometrically consistent, geometrically accurate, and noise-reduced images that clearly distinguished flooded areas from the surrounding landscape. This improved image quality enabled the threshold-based binarization to accurately separate flooded and non-flooded pixels, resulting in the well-defined flood extent maps shown in Figure 4, which formed the basis for subsequent flood extent calculation, spatial analysis, and impact assessment.

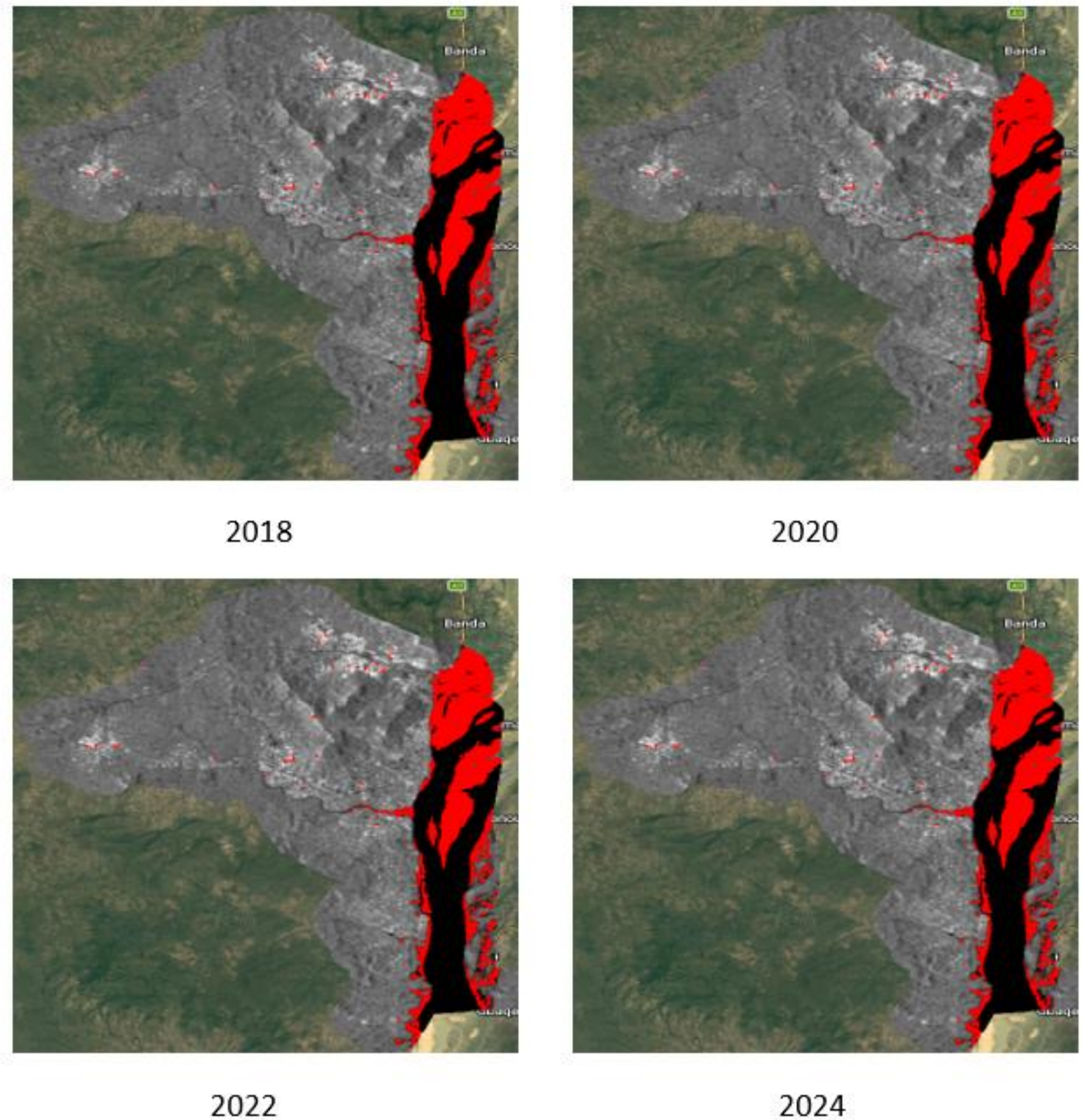

Figure 4. Delineated flood extents after threshold binarization

The total flood area for each of the years studied was calculated in ArcGIS Pro. Details are presented in Table 3

Table 3. Flood extent Area in square Km

Year	Flood extent Area (square Km)
2018	24.2
2020	12.75
2022	18.24
2024	18.09

ISSN 2682-681X (Paper), ISSN 2705-4241 (Online) | http://unilorinjoger.com | https://doi.org/10.63745/jogersi.2026.06.30.005

The extracted flood extents were stacked in ArcGIS Pro to produce a flood density map, as shown in Figure 6. Stacking the flood maps produces a composite map that enables the identification of flood hotspots (areas that are frequently flooded) and cold spots (areas that have never been flooded)

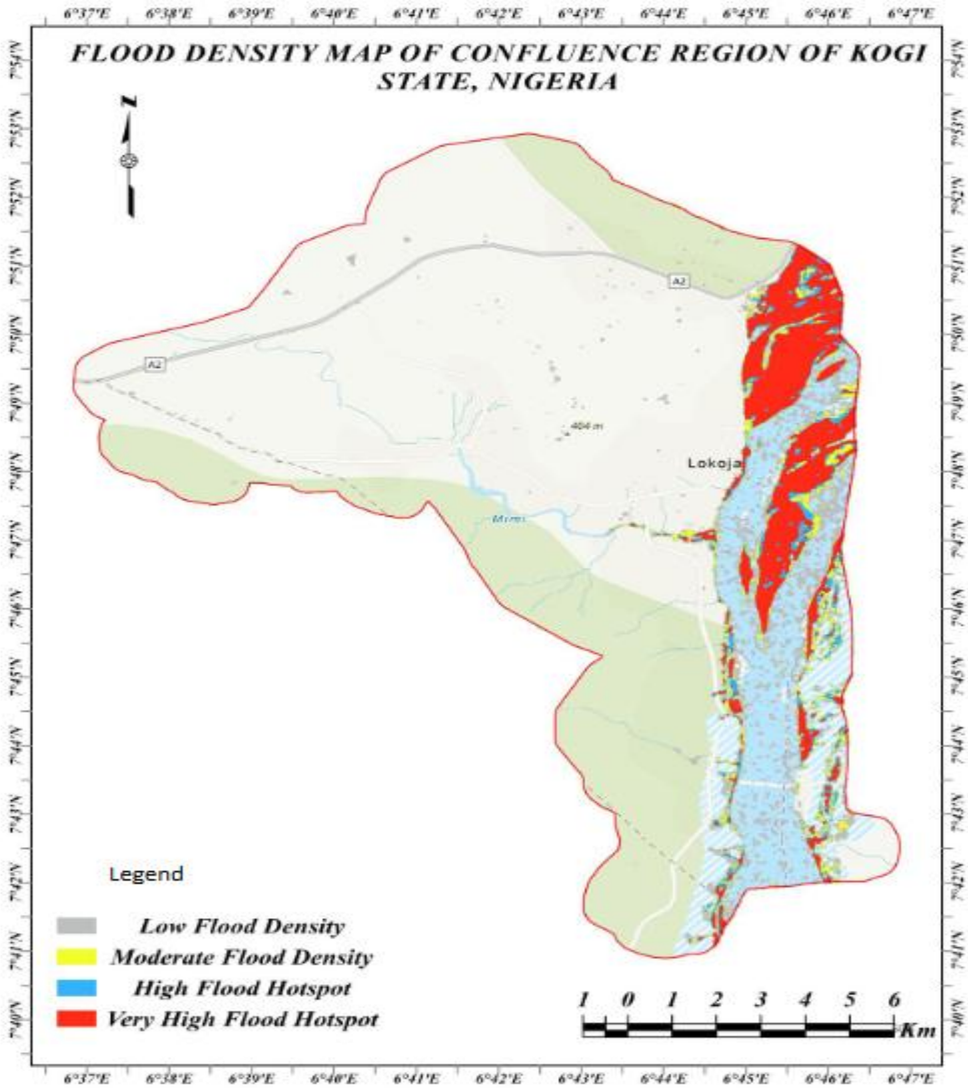

Figure 5. Flood density of the study area

3.2 Spatiotemporal pattern of Flooding (2018 to 2024)

The spatial pattern of flooding was assessed using Moran's I spatial autocorrelation statistic. Findings reveal that all the years assessed (2018, 2020, 2022, and 2024) had a Moran's I value very close to 1 (0.90, 0.88, 0.92, and 0.93) and a P-value less than 0.01 (0.0001, 0.0010, 0.0002, and 0.0001), indicating a strong clustering of similar values and positive auto-correlation. Details of Moran's I spatial statistics results for all the years considered are presented in Figure 7.

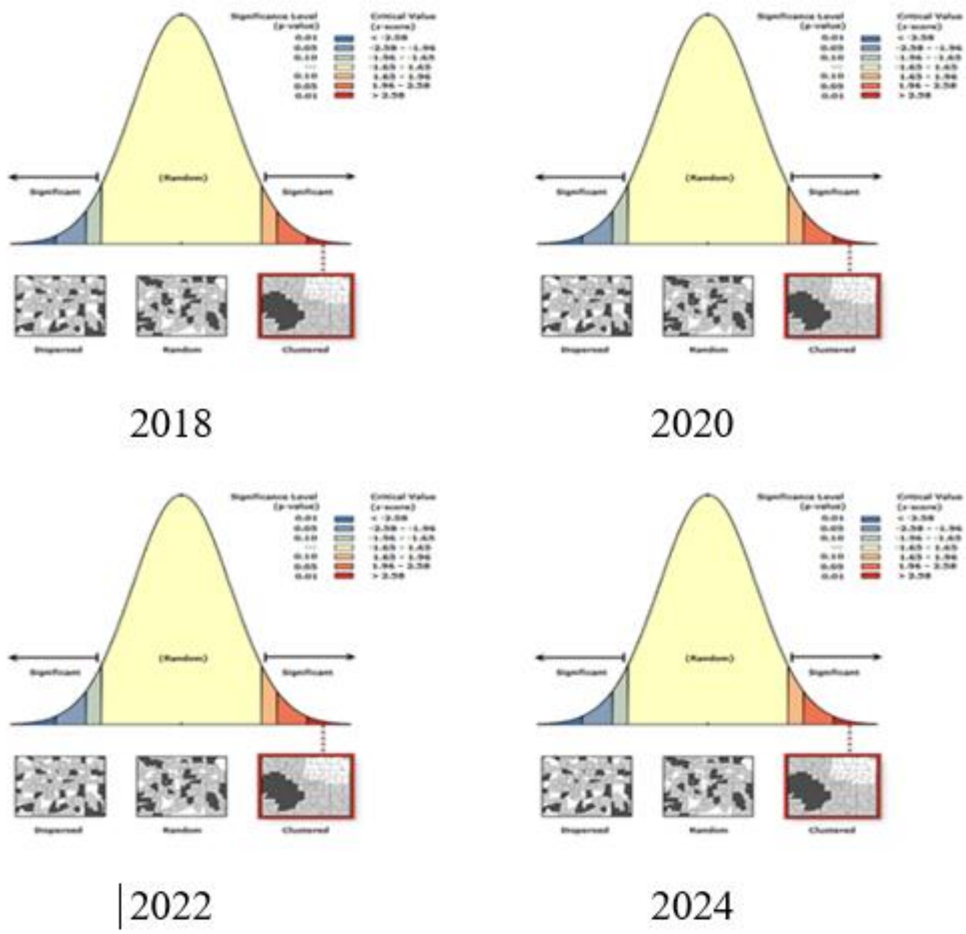

Figure 6: Spatial pattern of flooding in the study area visualized using Global Moran's I

3.3 Flood impact assessment

To assess the impact of flooding in the study area from 2018 to 2024, the flood maps were overlaid on land use land cover maps as shown in Figure 7. The results show that the 2018 flood event affected several farmlands and some built-up areas close to the banks of the River Niger. However, in 2020, while flooding was severe in farmlands, that in built-up areas was not as severe as in 2018. Furthermore, for all the years studied, some isolated flood cases were observed in built-up areas in Fiele town.

3.4 Validation of Results

The delineated flood extents showed strong agreement with documented flood events reported by the Nigerian Hydrological Services Agency (NIHSA), the National Emergency Management Agency (NEMA), and other published studies on flooding in the Niger–Benue confluence region. Historical records consistently identify Lokoja and adjoining communities within Bassa, Kogi, Ajaokuta, and Adavi Local Government Areas as among the most severely affected locations during the major flood events of 2018, 2020, 2022, and 2024 (NIHSA, 2023; Jimoh, 2022; Ohunene *et al*., 2025). These reported flood-prone areas correspond closely with the inundated zones delineated from the Sentinel-1 SAR imagery.

Field observations further confirmed that floodwaters were predominantly concentrated along the River Niger and River Benue floodplains, extending into adjacent agricultural lands and low-lying settlements. This observation is consistent with the flood extent maps, which show that inundation was largely confined to areas immediately surrounding the major river channels, while higher-elevation areas remained largely unaffected. In addition, the overlay analysis revealed that farmlands and built-up areas situated close to the

riverbanks experienced the greatest flood impacts, which agrees with field observations and documented reports of recurrent flooding and agricultural losses within the study area.
Furthermore, the flood hotspot areas identified through the flood density analysis correspond with locations historically recognized as repeatedly affected by seasonal flooding. Communities within the Niger–Benue floodplain have experienced recurrent inundation due to river overflow, prolonged rainfall, and upstream discharge, and these persistent flood-prone locations were similarly identified by the multi-temporal SAR analysis conducted in this study. The strong agreement between the extracted flood maps, historical flood reports, and field observations provides confidence in the reliability of the adopted Sentinel-1 SAR-based flood mapping methodology for accurately delineating flood extent in the confluence region of Kogi State.

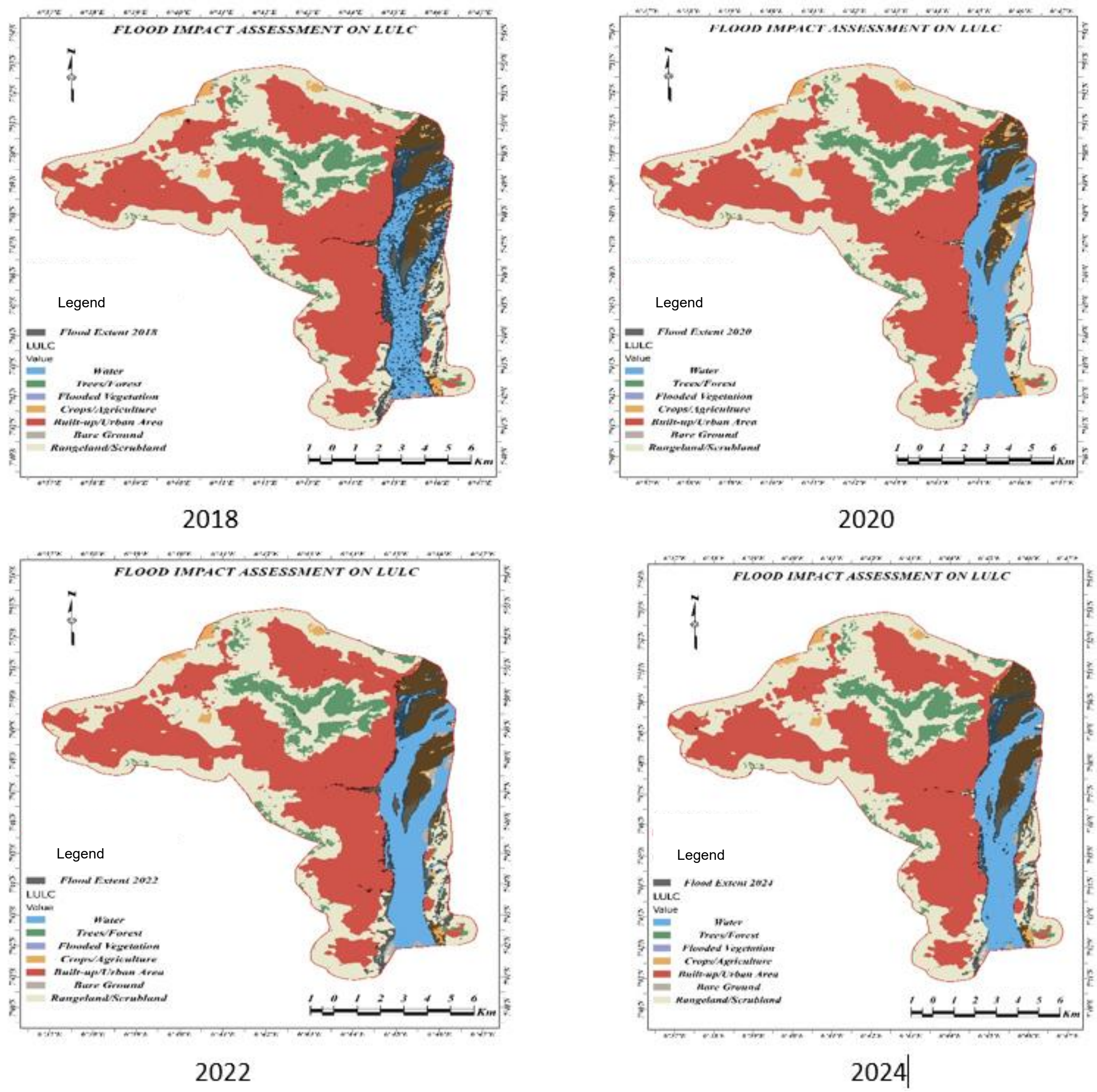

Figure 7. Flood maps overlaid on land use land cover maps to assess the impact of flooding on the study area from 2018 to 2024.

4.0 DISCUSSION

The findings of this study demonstrate the effectiveness of Sentinel-1 Synthetic Aperture Radar (SAR) imagery for detecting and mapping flood inundation within the confluence region of Kogi State. By integrating SAR image preprocessing, threshold-based image binarization, and GIS-based spatial analysis, the study successfully delineated flood extents for the 2018, 2020, 2022, and 2024 flood events despite the persistent cloud cover that typically accompanies major flood disasters. This confirms the suitability of Sentinel-1 SAR for operational flood monitoring under all-weather conditions, as similarly reported by Twele *et al*. (2016), Lang *et al*. (2024), and Sajid *et al*. (2025).

4.1 Variation in Flood Extent

The flood extent analysis revealed considerable temporal variability in inundation across the investigated flood years. Among the four events, the 2018 flood recorded the largest inundated area (24.20 km²), followed by the 2022 (18.24 km²), 2024 (18.09 km²), and 2020 (12.75 km²) flood events. These differences demonstrate that flood occurrence within the Niger–Benue confluence is highly dynamic and varies considerably from one event to another. The larger inundation observed during 2018 is consistent with reports that identified the 2018 flood as one of the most severe flood events experienced in the Niger–Benue Basin after the catastrophic 2012 flood. The extensive inundation during this period was primarily attributed to prolonged rainfall, high upstream discharge from the Niger and Benue Rivers, and increased reservoir releases, all of which contributed to widespread river overflow and floodplain inundation (UNDP, 2023; NIHSA, 2023).

Although the 2022 and 2024 flood events covered smaller areas than the 2018 event, both still produced substantial inundation within the study area. The similarity between the flood extents recorded in 2022 (18.24 km²) and 2024 (18.09 km²) suggests that flooding within the confluence region has remained consistently severe in recent years despite annual hydrological variations. This persistent occurrence reflects the increasing influence of climate variability, recurrent extreme rainfall events, catchment saturation, and upstream hydrological processes within the Niger–Benue River Basin. Conversely, the relatively smaller flood extent observed in 2020 may indicate comparatively lower river discharge, reduced rainfall intensity, or less extensive floodplain overflow during that event. Overall, these temporal differences highlight the necessity for continuous flood monitoring rather than relying on historical flood records alone, since flood magnitude varies significantly between years.

4.2 Spatial Pattern of Flooding

Spatial autocorrelation analysis further demonstrated that flooding within the study area exhibits a highly clustered spatial pattern rather than a random distribution. Moran's I values ranging from 0.88 to 0.93, coupled with statistically significant p-values (<0.01), indicate strong positive spatial autocorrelation for all investigated flood events. This implies that flooded pixels tend to occur in contiguous clusters concentrated within particular portions of the study area rather than being evenly distributed across the landscape.

The observed clustering is strongly influenced by the physical characteristics of the Niger–Benue confluence. Large sections of the study area consist of extensive floodplains, low-relief terrain, and settlements located immediately adjacent to major river channels. Such geomorphological conditions facilitate lateral expansion of floodwaters whenever river discharge exceeds channel capacity. Consequently, inundation repeatedly occurs along the same floodplain environments, producing persistent flood hotspots throughout successive flood events. Similar clustering behaviour has been reported in other riverine floodplains where topography, river morphology, and hydrological connectivity govern flood propagation and spatial concentration (Wang *et al*., 2022; Jimoh, 2022).

The flood density analysis further supports these findings by identifying locations repeatedly affected by flooding throughout the study period. Areas exhibiting high flood density represent chronic flood-prone zones where inundation occurred during multiple flood events, while locations with low flood density experienced flooding only under more extreme hydrological conditions. Such information provides valuable evidence for identifying long-term flood hotspots that require priority attention during flood mitigation planning, infrastructure development, and emergency preparedness. The identification of these recurrent flood zones demonstrates the usefulness of integrating multi-temporal SAR observations with GIS analysis for understanding flood persistence beyond individual flood events.

4.3 Flood Impact Assessment

Overlay analysis between the delineated flood maps and land use/land cover data revealed that flooding predominantly affected agricultural lands and built-up areas situated close to the River Niger. Farmlands constituted the most extensively inundated land-use category throughout the investigated years, reflecting the concentration of agricultural activities within fertile alluvial floodplains. Although these floodplains provide productive agricultural land due to nutrient-rich sediments, their repeated inundation exposes farming communities to substantial crop losses, reduced agricultural productivity, and economic hardship. This finding agrees with previous studies conducted within the Niger–Benue Basin, which identified agriculture as one of the sectors most vulnerable to recurrent flooding.

The analysis also revealed significant impacts on built-up areas, particularly during the 2018 flood event, when floodwaters extended into settlements located along the riverbanks. Residential communities, transportation infrastructure, and commercial facilities situated within these low-lying areas are therefore exposed to recurring flood hazards. Although built-up inundation was comparatively less extensive during the 2020 event, isolated flooding remained evident within settlements such as Fiele Town across multiple years, indicating persistent local vulnerability. These recurring impacts suggest that continued urban expansion into flood-prone environments may further increase exposure unless appropriate land-use regulations and flood-resilient planning measures are implemented.

The flood maps produced in this study provide spatially explicit information capable of supporting flood hazard zoning, infrastructure planning, evacuation planning, agricultural risk assessment, and the prioritization of structural and non-structural mitigation measures. Furthermore, the identified flood hotspots could guide government agencies in implementing targeted interventions such as floodplain management, improved drainage systems, flood-resilient infrastructure, early warning systems, and restrictions on future development within highly susceptible areas.

5.0 CONCLUSION

This study demonstrated the effectiveness of Sentinel-1 Synthetic Aperture Radar (SAR) imagery for detecting and mapping flood inundation in the confluence region of Kogi State, Nigeria. Through SAR image preprocessing, threshold-based image binarization, and GIS-based spatial analysis, the study successfully mapped the major flood events of 2018, 2020, 2022, and 2024. The results revealed significant temporal variations in flood extent, with the 2018 event recording the largest inundated area, while spatial autocorrelation and flood density analyses showed that flooding is highly clustered and recurrent along the Niger and Benue floodplains.

The flood impact assessment further revealed that agricultural lands and settlements located near the river channels are the most vulnerable to recurrent flooding. Overall, the study demonstrates that Sentinel-1 SAR provides a reliable and efficient tool for all-weather flood monitoring and generates valuable geospatial information for flood hazard assessment, land-use planning, and disaster risk management. By identifying recurrent flood hotspots and vulnerable areas, the findings provide an important basis for enhancing flood resilience through targeted mitigation measures, improved urban planning, early warning systems, and evidence-based decision-making.

Acknowledgments

The authors sincerely thank the Department of Surveying and Geoinformatics, University of Ilorin, for providing the facilities used in this study. The authors also appreciate the contribution of Dr. Mohammed Idrees for guidance and improvement of the research, and all individuals and institutions that supported this research.

Author Contributions

Conceptualization: H.A.A; Methodology: H.A.A.; Data curation: H.A.A.; Formal analysis: H.A.A. Writing—original draft: H.A.A; Writing—review and editing: H.A.A., A.B., and O.O.A..; Supervision: A.B. and O.O.A.

Disclosure Statement

The authors declare that there are no conflicts of interest regarding the publication of this paper. The research was conducted solely for academic and scientific purposes as part of the doctoral research activities of the first author within the Department of Surveying and Geoinformatics.

REFERENCES

Acosta-Coll, M., Ballester-Merelo, F., Martinez-Peiró, M., & De La Hoz-Franco, E. (2018). Real-Time Early Warning System Design for Pluvial Flash Floods—A Review. *Sensors*, *18*(7), 2255. https://doi.org/10.3390/s18072255

Alabi, M. O. (2012). *Urban landscape planning and soil variation in Nigeria: Lokoja as a case study*. Canadian Social Science, 8(5), 105–110. https://doi.org/10.3968/j.css.1923669720120805.1090

Ayuba, R.; Tijani, M.N. (2021). Hydrochemical characterization of groundwater in Lokoja, North-Central Nigeria. *Sustain. Water Resour. Manag.*, *7*, 61.

Bhola, P. K., Leandro, J., & Disse, M. (2020). Building Hazard Maps with Differentiated Risk Perception for Flood Impact Assessment. *Natural Hazards and Earth System Sciences*, *20*(10), 2647–2663. https://doi.org/10.5194/nhess-20-2647-2020

Chen, Y. (2021). An analytical process of spatial autocorrelation functions based on Moran's index. *PloS One*, *16*(4), e0249589.

Chen, Y. (2023). Spatial autocorrelation equation based on Moran's index. *Scientific Reports*, *13*(1), 19296.

Chlumsky, R., Craig, J. R., & Tolson, B. A. (2025). A Reach-Integrated Hydraulic Modelling Approach for Large-Scale and Real-Time Inundation Mapping. *Geoscientific Model Development*, *18*(11), 3387–3403. https://doi.org/10.5194/gmd-18-3387-2025

Destefanis, T., Guliyeva, S., Boccardo, P., & Fissore, V. (2025). Advancing Flood Detection and Mapping: A Review of Earth Observation Services, 3D Data Integration, and AI-Based Techniques. *Remote Sensing*, *17*(17), 2943. https://doi.org/10.3390/rs17172943

Ekene, E. P., Salubi, O. A., & Ohwoghere-Asuma, O. (2025). Flood risk assessment and zoning for Niamey and Lokoja metropolises in Niger and Nigeria. *Hydrology, 12*(1), 17.

European Space Agency (ESA). (2023). *Sentinel-1 Product Specification*. ESA.

Filipponi, F. (2019). Sentinel-1 GRD Preprocessing Workflow. *3rd International Electronic Conference on Remote Sensing*, 11. https://doi.org/10.3390/ECRS-3-06201

Gonzalez, R. C., & Woods, R. E. (2018). *Digital image processing* (4th ed.). Pearson.

Hategekimana, Y., Mukanyandwi, V., Kwizera, G., Karamage, F., Ntawukuriryayo, E., Manzi, F., Rwanyiziri, G., & Busogi, M. (2026). Modeling Flood Susceptibility in Rwanda Using an AI-Enabled Risk Mapping Tool. *Earth*, *7*(2), 53. https://doi.org/10.3390/earth7020053

Jimoh, U. U. (2022). Spatial and Seasonal Patterns of Flood Inundation in Lokoja, Kogi State, Nigeria. *Forum Geografi*, *36*(1). https://doi.org/10.23917/forgeo.v36i1.15968

Jong-Sen Lee, Jen-Hung Wen, Ainsworth, T. L., Kun-Shan Chen, & Chen, A. J. (2009). Improved Sigma Filter for Speckle Filtering of SAR Imagery. *IEEE Transactions on Geoscience and Remote Sensing*, *47*(1), 202–213. https://doi.org/10.1109/TGRS.2008.2002881

Kaçmaz, A., & Alganci, U. (2026). SAR-Based Flood Extent Mapping with a Lightweight Siamese U-Net and Differential Attention Mechanism. *Earth*, *7*(3), 87. https://doi.org/10.3390/earth7030087

Kumar, V., Sharma, K., Caloiero, T., Mehta, D., & Singh, K. (2023). Comprehensive Overview of Flood Modeling Approaches: A Review of Recent Advances. *Hydrology*, *10*(7), 141. https://doi.org/10.3390/hydrology10070141

Kumari, M., Sarma, K., & Sharma, R. (2019). Using Moran's I and GIS to study the spatial pattern of land surface temperature in relation to land use/cover around a thermal power plant in Singrauli district, Madhya Pradesh, India. *Remote Sensing Applications: Society and Environment*, *15*, 100239.

Lang, F., Zhu, Y., Zhao, J., Hu, X., Shi, H., Zheng, N., & Zha, J. (2024). Flood Mapping of Synthetic Aperture Radar (SAR) Imagery Based on Semi-Automatic Thresholding and Change Detection. *Remote Sensing*, *16*(15), 2763. https://doi.org/10.3390/rs16152763

Martinis, S. (2010). *Automatic Near Real-Time Flood Detection in High Resolution X-Band Synthetic Aperture Radar Satellite Data Using Context-Based Classification on Irregular Graphs*.

Mason, D. C., & Dance, S. L. (2026). Improved Urban Flood Detection Using Sentinel-1 by Effective Combination of Elevation Data with Image Intensity and Interferometric Coherence. *Journal of Applied Remote Sensing*, *20*(02). https://doi.org/10.1117/1.JRS.20.026510

Mazarakis, V., Tsanakas, K., Greenbaum, N., Batzakis, D.-V., Sorrentino, A., Tsodoulos, I., Valkanou, K., & Karymbalis, E. (2025). Flood-Hazard Assessment in the Messapios River Catchment (Central Evia Island, Greece) by Integrating GIS-Based Multi-Criteria Decision Analysis and Analytic Hierarchy Process. *Land*, *14*(3), 658. https://doi.org/10.3390/land14030658

Nazir, M. F., Atif, S., & Hussain, E. (2025). An integrated geographic information system (GIS) and analytical hierarchy process (AHP)-based approach for drone-optimized large-scale flood imaging. *Drone Systems and Applications*, *13*, 1–18. https://doi.org/10.1139/dsa-2024-0039

Nigerian Hydrological Services Agency (NIHSA). (2023). *Annual flood outlook (AFO) 2023*. Abuja, Nigeria: Federal Ministry of Water Resources.

Ohunene, I., Adewuyi, T., Garba, A., Mbow, C., Agbaje, G., Rufus, O., & Monsor, O. (2025). Assessing Nature-Based Flood Mitigation Measures at the General Area of the Confluence of Rivers Benue and Niger in Kogi State, Nigeria. *American Journal of Remote Sensing*, *13*(1), 13–31. https://doi.org/10.11648/j.ajrs.20251301.12

Okosun, S. E., Patrick, R. A., & Banki, T. C. (2025). Assessment of Flood Menace: A Perspective from Lokoja Communities of Kogi State, Nigeria. *Journal of Inclusive Cities and Built Environment*, *5*(8), 45–57.

Patricia, A., Yisaga, D., Akpegi Onah, M., Adimanyi, O., & Grace Stephen, E. (2024). Time Series Analysis of River Discharge, Water Stage, and Rainfall at Lokoja Section of Benue River, Kogi State, Nigeria. *Journal of Environmental Science and Agricultural Research*, 1–8. https://doi.org/10.61440/JESAR.2024.v2.31

Rahman, M. R., Kang, S., Lee, S., & Lee, J. (2025). A green infrastructure planning approach for enhanced flood control and resilience in urban areas. *Land Use Policy*, *153*, 107535. https://doi.org/10.1016/j.landusepol.2025.107535

Sajid, M., Khan, H. H., Khan, A., Ahmad, R., Khan, A., Siraj, G., & Ansari, A. A. (2025). Application of Sentinel-1 SAR Data for Flood Monitoring in the Lower Ganges Basin: A Time-Series Analysis of 2021 Flood in Bihar. *Discover Sensors*, *1*(1), 12. https://doi.org/10.1007/s44397-025-00012-2

Samela, C., Coluzzi, R., Imbrenda, V., Manfreda, S., & Lanfredi, M. (2022). Satellite Flood Detection Integrating Hydrogeomorphic and Spectral Indices. *GIScience & Remote Sensing*, *59*(1), 1997–2018. https://doi.org/10.1080/15481603.2022.2143670

Sampson, C. C., Smith, A. M., Bates, P. D., Neal, J. C., Alfieri, L., & Freer, J. E. (2015). A High-Resolution Global Flood Hazard Model: A HIGH-RESOLUTION GLOBAL FLOOD HAZARD MODEL. *Water Resources Research*, *51*(9), 7358–7381. https://doi.org/10.1002/2015WR016954

Shuaibu, A., Hounkpè, J., Bossa, Y. A., & Kalin, R. M. (2022). Flood Risk Assessment and Mapping in the Hadejia River Basin, Nigeria, Using Hydro-Geomorphic Approach and Multi-Criterion Decision-Making Method. *Water*, *14*(22), 3709. https://doi.org/10.3390/w14223709

Tang, X., Du, J., Zhou, H., Hu, Z., Liu, B., & Hu, M. (2026). Systematic Review for Urban Flood Disaster in Managerial Perspective: Forecasting, Assessment and Optimization. *Sustainability*, *18*(2), 1106. https://doi.org/10.3390/su18021106

Twele, A., Cao, W., Plank, S., & Martinis, S. (2016). Sentinel-1-based flood mapping: A fully automated processing chain. *International Journal of Remote Sensing*, *37*(13), 2990–3004. https://doi.org/10.1080/01431161.2016.1192304

Venter, Z. S., & Sydenham, M. A. K. (2021). Continental-Scale Land Cover Mapping at 10 M Resolution Over Europe (ELC10). *Remote Sensing*, *13*(12), 2301. https://doi.org/10.3390/rs13122301

Wagner, W., Bauer-Marschallinger, B., Roth, F., Raiger-Stachl, T., Reimer, C., McCormick, N., Matgen, P., Chini, M., Li, Y., Martinis, S., Wieland, M., Kraft, F., Festa, D., Hassaan, M., Tupas, M. E., Zhao, J., Seewald, M., Riffler, M., Molini, L., … Salamon, P. (2026). The fully-automatic Sentinel-1 Global Flood Monitoring service: Scientific challenges and future directions. *Remote Sensing of Environment*, *333*, 115108. https://doi.org/10.1016/j.rse.2025.115108

Wang, C., Ke, J., Xiu, W., Ye, K., & Li, Q. (2019). Emergency Response Using Volunteered Passenger Aircraft Remote Sensing Data: A Case Study on Flood Damage Mapping. *Sensors*, *19*(19), 4163. https://doi.org/10.3390/s19194163

Wang, L., Cui, S., Li, Y., Huang, H., Manandhar, B., Nitivattananon, V., Fang, X., & Huang, W. (2022). A Review of the Flood Management: From Flood Control to Flood Resilience. *Heliyon*, *8*(11), e11763. https://doi.org/10.1016/j.heliyon.2022.e11763

Wang, Y., Lv, W., Wang, M., Chen, X., & Li, Y. (2023). Application of improved Moran's I in the evaluation of urban spatial development. *Spatial Statistics*, *54*, 100736.

Zhou, Y., Chen, X., Yin, Q., Ma, F., & Zhang, F. (2025). SAR Radiometric Cross-Calibration Based on Multiple Pseudoinvariant Calibration Sites With Extensive Backscattering Coefficient Range. *IEEE Journal of Selected Topics in Applied Earth Observations and Remote Sensing*, *18*, 4836–4849. https://doi.org/10.1109/JSTARS.2025.3525461